

Searches for beyond the Standard Model Higgs Bosons at ATLAS

M. WARSINSKY on behalf of the ATLAS COLLABORATION

*Albert-Ludwigs-Universität Freiburg, Physikalisches Institut - Hermann-Herder-Str. 3
D-79104 Freiburg, Germany*

ricevuto il 7 Settembre 2012

Summary. — Searches for beyond the Standard Model Higgs bosons with the ATLAS detector at the Large Hadron Collider are presented. The individual results are based on datasets with integrated luminosities between 35 pb^{-1} and 1.6 fb^{-1} of proton-proton collisions at a centre-of-mass energy of 7 TeV. No significant deviation from Standard Model predictions without a Higgs boson are observed. Exclusion limits are set on production cross-sections as a function of the Higgs boson mass and in the parameter space of supersymmetric models.

PACS 14.80.Da – Supersymmetric Higgs bosons.

PACS 14.80.Fd – Other charged Higgs bosons.

PACS 12.60.Fr – Extensions of electroweak Higgs sector.

1. – Introduction

One of the primary goals of the ATLAS experiment [1] at the Large Hadron Collider (LHC) is to probe the mechanism responsible for electroweak symmetry breaking and the origin of mass of elementary particles. In the Standard Model (SM) [2] electroweak symmetry breaking is accomplished by adding an additional complex $SU(2)$ doublet field which acquires a vacuum expectation value [3]. A direct prediction of this mechanism is the existence of one additional massive scalar particle, the Higgs boson [3], which couples to both fermions and bosons with coupling strengths that are directly predicted by the theory, with the only unknown quantity being the mass of the Higgs boson. Results from the ATLAS experiment on searches for a SM-like Higgs boson can be found in [4].

Extensions of the Standard Model can significantly alter the phenomenology of the Higgs sector, thus requiring additional search strategies in order to ensure a discovery. Among the possible extensions of the SM, one of the most popular ones is the Minimal Supersymmetric Standard Model (MSSM) [5], where an additional Higgs doublet field of opposite hypercharge is required. This results in five observable Higgs bosons, three of them being electrically neutral (the CP -even h, H , the CP -odd A), and two being charged (H^\pm). In addition the coupling strengths to fermions and bosons of the neutral

Higgs bosons can be very different from the SM case. Further extensions of the SM gauge sector, such as left-right-symmetric models [6], Higgs triplet models [7], and little Higgs models [8] predict the existence of doubly charged Higgs bosons. Models like the next-to-minimal supersymmetric standard model (NMSSM) [9] can lead to an even more complex Higgs sector. Finally, fermiophobic models [10] can cause the Higgs boson to not couple to some or all of the SM fermions.

In these proceedings, ATLAS results from searches for Higgs bosons in scenarios beyond the Standard Model are reported.

2. – Neutral MSSM $h/H/A \rightarrow \tau\tau$

In the MSSM the coupling strength of the neutral Higgs bosons to fermions and gauge bosons is significantly altered. For large values of $\tan\beta$ one of the two CP -even Higgs bosons is always predicted to have about the same mass as the A boson and these two mass degenerate states will have increased couplings to down-type fermions, while the couplings to gauge bosons will be suppressed or even completely absent in the case of the A boson. The other CP -even Higgs boson has couplings similar to the SM case.

The two mass degenerate Higgs bosons are produced predominantly in gluon-gluon-fusion and in association with b quarks. Decay to down-type fermions are favoured, with branching fractions of about 90% into $b\bar{b}$ and about 10% into $\tau^+\tau^-$. The latter decay mode is one of the most promising channels. However, it is difficult to reconstruct the Higgs boson mass due to the presence of neutrinos in the tau lepton decays, and the large jet background to hadronic tau lepton decays (τ_h) has to be suppressed.

In ATLAS the search for neutral Higgs bosons of the MSSM has been performed in a jet-inclusive way based on the decay of the Higgs bosons into tau leptons using 1.06 fb^{-1} of data [11]. Four different final states according to decays of tau leptons have been considered, with τ_h denoting a tau lepton decay involving hadrons, $e\mu 4\nu$, $e\tau_h 3\nu$, $\mu\tau_h 3\nu$, $\tau_h\tau_h 2\nu$, corresponding to branching fractions of 6%, 23%, 23% and 42% respectively⁽¹⁾. Various estimates for the invariant mass of the Higgs boson candidate have been used: In the $\tau_h\tau_h$ channel the invariant (also called visible) mass of the two hadronic systems has been used. For the $e\mu$ channel, the missing momentum was added to the visible tau decay products to produce an effective mass. For the channels with one leptonic and one hadronic tau lepton decay the missing mass calculator (MMC) technique as introduced in [12] has been used.

For channels with leptons in the final state the dominant background $Z \rightarrow \tau\tau$ has been estimated from data with a technique where $Z \rightarrow \mu\mu$ events are selected in data. The muons are removed from the event and their momenta used as momenta of fictitious tau leptons. The tau lepton decays are simulated along with the detector response and the simulated energy deposits are re-merged with the data event before re-reconstruction. In this way the additional hadronic activity in the event is taken from data.

For the $\tau_h\tau_h$ channel the dominant background is multi-jet production, which has been estimated from data. Details on the analysis can be found in [11].

Figure 1 shows the resulting mass spectra of the three different channels. Data are compatible with background expectations for all channels and exclusion limits at the 95% CL are set on the production cross-section times branching fraction of a generic scalar resonance ϕ as a function of its mass as shown in fig. 2 (left). The cross-section

⁽¹⁾ In the following the $e\tau_h$ and $\mu\tau_h$ channels will be summarized as one $\ell\tau_h$ channel.

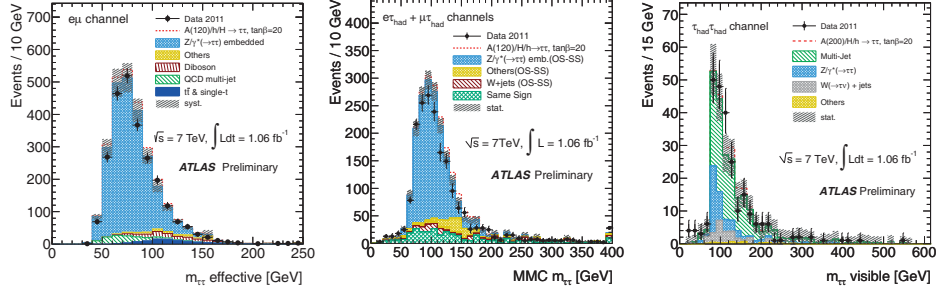


Fig. 1. – Reconstructed masses in the search for $h/H/A \rightarrow \tau\tau$ using 1.06 fb^{-1} [11]. From left to right: Effective mass in the $e\mu$ channel, MMC mass in the $\ell\tau_h$ channels, visible mass in the $\tau_h\tau_h$ channel.

limit is produced separately for two different production mechanisms, $gg \rightarrow \phi$ and b quark associated production. The interpretation of the search results within the MSSM is shown in fig. 2 (right), where the exclusion limits are set on $\tan\beta$ as a function of the mass of the CP -odd Higgs boson A . Here the MHMAX [13] scenario has been assumed.

3. – Searches for charged Higgs bosons

Charged Higgs bosons occur in all extensions of the SM Higgs sector with more than one Higgs doublet field, such as the MSSM. In all analysis presented in these proceedings, a charged Higgs boson mass smaller than the top quark mass is assumed and the charged Higgs boson is searched for in decays of top quark pairs ($t\bar{t} \rightarrow H^+bW^- \bar{b} + \text{c.c.}$).

3.1. Charged $H^+ \rightarrow \tau^+\nu_\tau$. – The decay of the charged Higgs boson into tau leptons is important in the MSSM especially for large values of $\tan\beta$. The search for this decay channel has been performed in three different final states using 1.03 fb^{-1} of data. Details

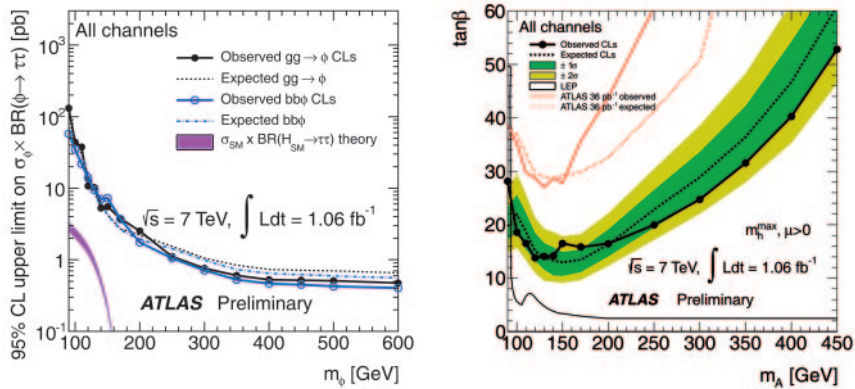


Fig. 2. – Expected and observed exclusion limits at the 95% CL from the combination of the analyses in the $e\mu$, $\ell\tau_h$ and $\tau_h\tau_h$ channels [11]. Left: Limits on production cross-section times branching fraction of a single scalar resonance decaying into $\tau\tau$. Right: Limits in the m_A - $\tan\beta$ plane of the MSSM in the MHMAX scenario.

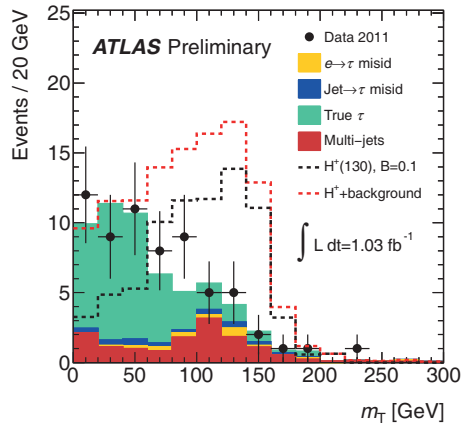


Fig. 3. – Transverse mass of the hadronic tau candidate and the missing transverse energy in the search for $H^+ \rightarrow \tau\nu$ for the analysis using hadronic tau lepton decays [14] using 1.03 fb^{-1} .

of the analysis for the case where both the tau lepton and the W boson from the second top quark decaying hadronically can be found in [14]. In [15] the analysis where either only the tau lepton decays leptonically or in addition also the W boson from the second top quark decays leptonically can be found.

In the hadronic channel, dominant backgrounds are top quark pairs and W +jets with real tau leptons, which are estimated using a data-driven technique where events are selected with a similar event topology as in the analysis, but requiring a reconstructed muon instead of a tau candidate. The reconstructed muon is removed from the event and replaced by a simulated tau lepton decaying hadronically, where the tau momentum is taken from the reconstructed muon. Fake tau lepton contributions are estimated by applying measured fake rates to simulation. The multi-jet background is estimated using control regions defined by inverting tau identification and b -tagging requirements.

The transverse mass of the tau candidate and the missing momentum is used as a final discriminant [14] and is shown in fig. 3. The observation is consistent with background expectations and upper limits are set on $BR(t \rightarrow H^+b) \cdot BR(H^+ \rightarrow \tau\nu)$, as shown in fig. 4 (left). This result can also be interpreted in the MSSM using the MHMAX [13] scenario as limits on the $\tan\beta$ in dependence of the mass of the charged Higgs boson, as shown in fig. 4 (right).

In the channels involving electrons or muons, the signal is enhanced by cutting on the invariant mass of the b -quark and the electron or muon coming from the same top quark decay. The final discriminating variables used are transverse masses obtained by maximizing the invariant mass over all possible values of neutrino momenta in each event, as described in [16]. Also in these two channels the observation is consistent with background expectations [15]. Limits are set on $BR(t \rightarrow H^+b)$ assuming $BR(H^+ \rightarrow \tau\nu) = 1$ and on $\tan\beta$ in dependence of the charged Higgs boson mass in the MHMAX scenario [13] of the MSSM. The combined limit of the leptonic channels is shown in fig. 5.

Although the presence of leptons suppresses the backgrounds significantly, the higher statistics of hadronic tau decays leads to stronger limits from the hadronic channel than from the leptonic ones.

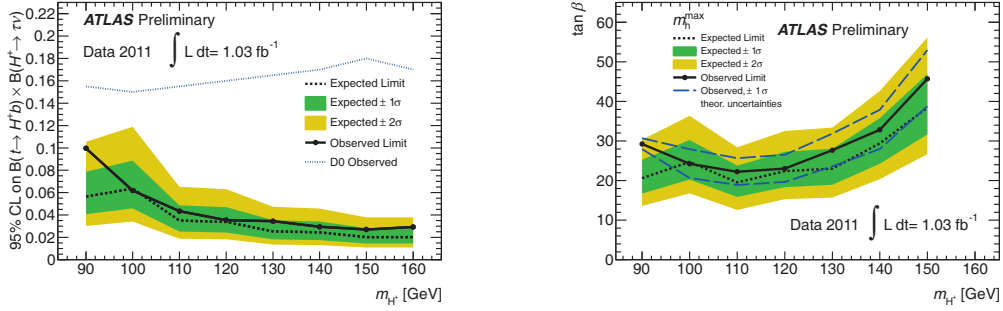


Fig. 4. – Expected and observed exclusion limits on the production of a charged Higgs boson in top quark decays in the hadronic channel [14] in dependence of the charged Higgs boson mass. Left: Limit on the branching fractions, right: limit on $\tan \beta$ using the MHMAX scenario of the MSSM.

3.2. Charged $H^+ \rightarrow c\bar{s}$. – A search for charged Higgs bosons in the $H^+ \rightarrow c\bar{s}$ using 35 pb^{-1} of data taken in 2010 is documented in detail in [17]. This decay mode is important for low values of $\tan \beta < 1$. The analysis makes use of an electron or muon from the decay of the W -boson emanating from the second top quark decay. The signal characteristic is similar to semi-leptonic $t\bar{t}$ events, with the exception of the invariant mass of the two jets from the H^+ decay, which peaks at m_{H^+} instead of m_W . A kinematic fit is performed to select the two jets originating from the H^+ candidate. Both the overall number of events and the shape of the di-jet mass distribution are found to be consistent with SM expectations. Limits are set on the branching fraction $BR(t \rightarrow H^+ b)$, assuming $BR(H^+ \rightarrow c\bar{s}) = 1$, see fig. 6.

4. – Search for a fermiophobic Higgs boson

Fermiophobic extensions of the Standard Model [10] can lead to suppressed or even absent couplings of the Higgs field to some or all fermion generations. In this way, both production and decay of the Higgs boson are altered significantly. In the ATLAS analysis reported in [18] the fermiophobic benchmark scenario [10] is assumed, where all Higgs

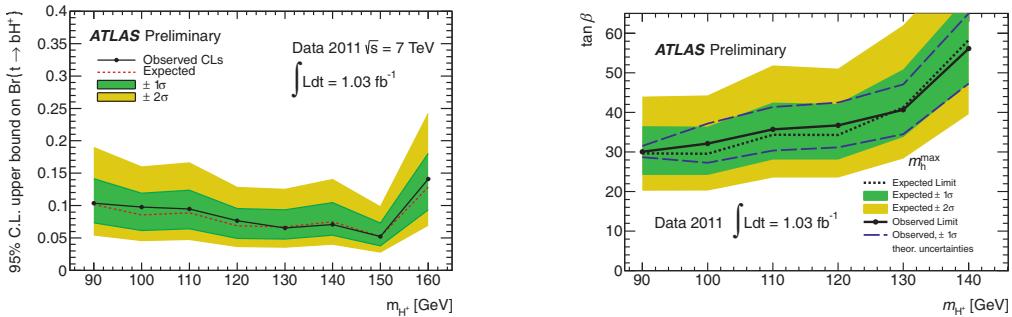


Fig. 5. – Expected and observed exclusion limits on the production of a charged Higgs boson in top quark decays in the leptonic channels [15] in dependence of the charged Higgs boson mass. Left: Limit on the branching fraction, right: limit on $\tan \beta$ using the MHMAX scenario of the MSSM.

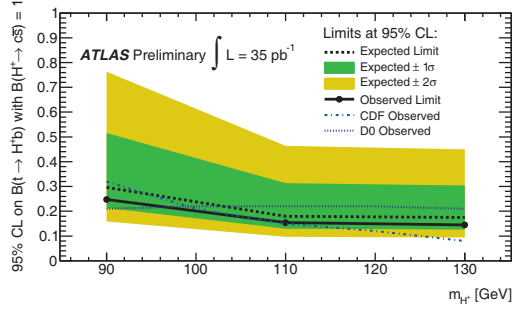


Fig. 6. – Expected and observed upper limit on the branching fraction $t \rightarrow H^+ b$ assuming only decays $H^+ \rightarrow c\bar{s}$ using a dataset of 35 pb^{-1} [17].

boson couplings to fermions are set to zero, but the couplings to gauge bosons are left at the Standard Model values. In this model the decay $H \rightarrow \gamma\gamma$ is strongly enhanced compared to the SM case, especially for low Higgs boson masses. The analysis follows the ATLAS Standard Model search for $H \rightarrow \gamma\gamma$ [4], using an integrated luminosity of 1.08 fb^{-1} . Two energetic isolated photons with transverse momenta of at least 40 GeV and 25 GeV are required. The background consists primarily of di-photon production and misidentified photon-jet events. As in comparison to the SM case the Higgs boson is produced only in vector-boson fusion and Higgsstrahlung production, it has on average a higher transverse momentum. This particular topology is employed to increase the sensitivity of the analysis by considering the di-photon invariant mass spectrum in three ranges of the transverse momentum of the fermion pair. The three resulting mass spectra are fitted simultaneously for Higgs boson mass hypotheses between 110 GeV and 130 GeV. No significant excess is observed, and the resulting exclusion limits are shown in fig. 7. The mass ranges 110–111 GeV and 113.5–117.5 GeV are excluded at the 95% CL.

5. – Search for doubly charged Higgs bosons

Doubly charged Higgs bosons are predicted by a number of extensions of the Standard Model, such as left-right symmetric models [6], Higgs triplet models [7] or little Higgs

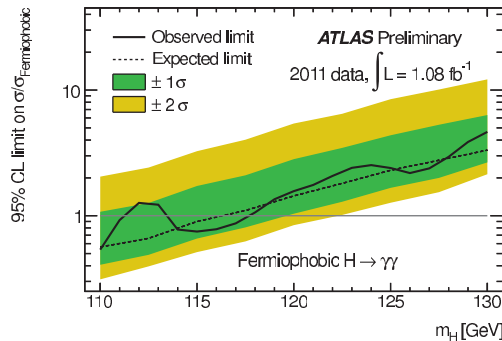


Fig. 7. – Exclusion limits at the 95% CL on the production rate of a fermiophobic Higgs boson normalized to the prediction of the fermiophobic benchmark scenario as a function of the Higgs boson mass hypothesis [18] using an integrated luminosity of 1.08 fb^{-1} .

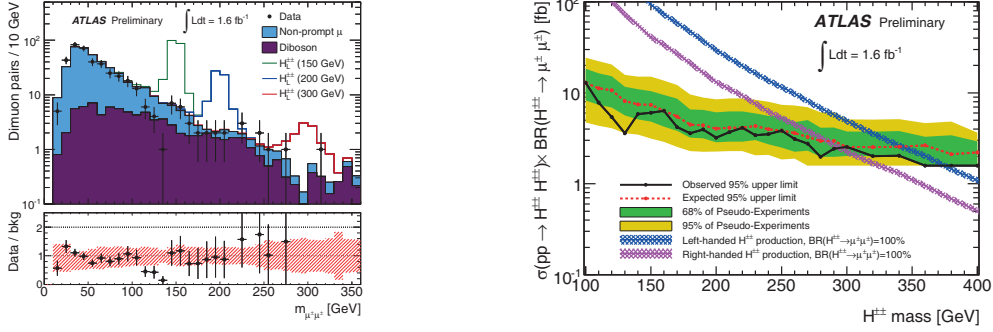


Fig. 8. – Results of the search for doubly charged Higgs bosons using 1.6 fb^{-1} of data [19]. Left: Invariant di-muon mass spectrum after selection cuts. Right: Upper limit at the 95% CL on the cross-section times branching fraction for pair production of doubly charged Higgs bosons decaying into muons.

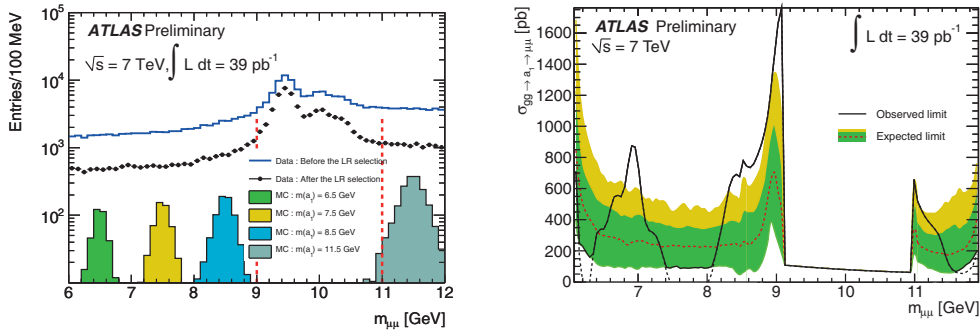


Fig. 9. – Left: Invariant di-muon mass spectrum for the search for $a_1 \rightarrow \mu\mu$ using a dataset of 39 pb^{-1} [21]. Right: Expected and observed exclusion limits on cross-section times branching fraction for $gg \rightarrow a_1 \rightarrow \mu\mu$ in dependence of the di-muon invariant mass [21].

models [8]. In proton-proton collisions, doubly charged Higgs bosons are dominantly produced in pairs via the Drell-Yann process $pp \rightarrow H^{++}H^{--}$. In a dataset with an integrated luminosity of 1.6 fb^{-1} , events with two muons with same electric charge are selected [19]. To ensure a short lifetime ($c\tau < 10 \mu\text{m}$) and a relative natural width of the doubly charged Higgs boson of less than 1%, only coupling values of the H^{++} to muons between 10^{-5} and 0.5 are considered. The resulting di-muon invariant mass spectrum as shown in fig. 8 (left) is in good agreement with background predictions. The main background at low masses arises from non-prompt muons from heavy flavour decays or decays in flight of pions or kaons. For high invariant masses di-boson production gives an additional contribution. Limits are set on the production cross-section of doubly charged Higgs bosons as shown in fig. 8 (right). Assuming a branching fraction of the doubly charged Higgs boson into muons of one, limits are set on the H^{++} mass of 295 GeV (375 GeV) for right-handed (left-handed) production⁽²⁾.

⁽²⁾ The production cross-section for left-handed production is a factor of two larger than for right-handed production.

6. – Search for NMSSM $a_1 \rightarrow \mu^+\mu^-$

The Next-to-MSSM (NMSSM) introduces an additional complex singlet scalar field to solve the so-called μ -problem [9]. As a consequence, the Higgs sector expands to three CP -even scalars ($h_1h_2h_3$), two CP -odd scalars (a_1, a_2) and two charged scalars (H^\pm). The light CP -odd scalar a_1 can be rather light, *i.e.* below the threshold to produce B -hadron pairs ($m_{a_1} < 2m_B$). As in [20] the direct production of the a_1 in gluon-gluon fusion and the decay into muons has been considered in the ATLAS analysis presented in [21]. The signal over background ratio is enhanced by cutting on a Likelihood ratio (LR) based on the dimuon vertex fit and on muon isolation variables. The obtained invariant mass spectrum is shown in fig. 9 (left). The region around the Υ resonances is excluded from the search. Exclusion limits on the production cross-section are shown in fig. 9 (right). Deviations of the observed limit from its expected value are consistent with statistical fluctuations without an additional resonance after taking into account look-elsewhere effects [22].

7. – Summary

The ATLAS experiment has probed a wide variety of possible extensions of the SM Higgs sector. Neutral and charged Higgs bosons within the MSSM, fermiophobic models in $H \rightarrow \gamma\gamma$, doubly charged Higgs bosons and also light Higgs bosons within the NMSSM have been probed. In all analyses presented, using data between 35 pb^{-1} and 1.6 fb^{-1} , the observations are compatible with background-only expectations. Stringent limits on production cross-sections and/or branching fractions have been set, and in part also been interpreted within the MSSM.

* * *

We acknowledge the support of the Initiative and Networking Fund of the Helmholtz Association, contract HA-101 (Physics at the Terascale).

REFERENCES

- [1] ATLAS COLLABORATION, *JINST*, **3** (2008) S08003.
- [2] GLASHOW S. L., *Nucl. Phys.*, **22** (1961) 579; WEINBERG S., *Phys. Rev. Lett.*, **19** (1967) 1264; SALAM A., *Conf. Proc. C*, **680519** (1968) 367.
- [3] HIGGS P. W., *Phys. Lett.*, **12** (1964) 132; *Phys. Rev. Lett.*, **13** (1964) 508; *Phys. Rev.*, **145** (1966) 1156; ENGLERT F. and BROUT R., *Phys. Rev. Lett.*, **13** (1964) 321; GURALNIK G. S., HAGEN C. R. and KIBBLE T. W. B., *Phys. Rev. Lett.*, **13** (1964) 585.
- [4] ATLAS COLLABORATION, *Phys. Lett. B*, **710** (2012) 49.
- [5] NILLES H. P., *Phys. Rep.*, **110** (1984) 1; HABER H. E. and KANE G. L., *Phys. Rep.*, **117** (1985) 75.
- [6] SENJANOVIC G. and MOHAPATRA R. N., *Phys. Rev. D*, **12** (1975) 1502.
- [7] GEORGI H. and MACHACEK M., *Nucl. Phys. B*, **262** (1985) 463; GUNION J. F., VEGA R. and WUDKA J., *Phys. Rev. D*, **42** (1990) 1673.
- [8] ARKANI-HAMED N. *et al.*, *JHEP*, **08** (2002) 021.
- [9] MANIATIS M., *Int. J. Mod. Phys. A*, **25** (2010) 3505.
- [10] LEP HIGGS WG and ALEPH, DELPHI, L3 and OPAL COLLABORATIONS, hep-ex/0107035.
- [11] ATLAS COLLABORATION, ATLAS-CONF-2011-132, <https://cdsweb.cern.ch/record/1383835>.

- [12] ELAGIN A., MURAT P., PRANKO A. and SAFONOV A., *Nucl. Instrum. Methods A*, **654** (2011) 481.
- [13] CARENA M. S., HEINEMEYER S., WAGNER C. E. M. and WEIGLEIN G., hep-ph/9912223.
- [14] ATLAS COLLABORATION, ATLAS-CONF-2011-138, <https://cdsweb.cern.ch/record/1383841>.
- [15] ATLAS COLLABORATION, ATLAS-CONF-2011-151, <https://cdsweb.cern.ch/record/1398187>.
- [16] GROSS E. and VITELLS O., *Phys. Rev. D*, **81** (2010) 055010.
- [17] ATLAS COLLABORATION, ATLAS-CONF-2011-094, <https://cdsweb.cern.ch/record/1367737>.
- [18] ATLAS COLLABORATION, ATLAS-CONF-2011-149, <https://cdsweb.cern.ch/record/1397815>.
- [19] ATLAS COLLABORATION, ATLAS-CONF-2011-127, <https://cdsweb.cern.ch/record/1383792>.
- [20] GUNION J. F., *JHEP*, **08** (2009) 032.
- [21] ATLAS COLLABORATION, ATLAS-CONF-2011-020, <https://cdsweb.cern.ch/record/1336749>.
- [22] LYONS L., *Ann. Appl. Stat.* 2008, Vol. 2, No. 3, 887-915; DEMORTIER L., *Proceedings of PHYSTAT-LHC Workshop 2007*, CERN-2008-001; GROSS E. and VITELLS O., *Eur. Phys. J. C*, **70** (2010) 525.